Journal of Electromagnetic Waves and Applications

ISSN: 0920-5071 (Print) 1569-3937 (Online) Journal homepage: http://www.tandfonline.com/loi/tewa20

A constant absolute bandwidth tunable band-pass filter based on magnetic dominated mixed coupling and source–load electric coupling

Dengyao Tian, Quanyuan Feng & Qianyin Xiang

JOURNAL OF ELECTROMAGNETIC WAVES AND APPLICATIONS, 2016
http://dx.doi.org/10.1080/09205071.2016.1226965

Taylor & Francis
Taylor & Francis Group

A constant absolute bandwidth tunable band-pass filter based on magnetic dominated mixed coupling and source–load electric coupling

Dengyao Tian, Quanyuan Feng and Qianyin Xiang

School of Information and Science Technology, Southwest Jiaotong University, Chengdu, China

ABSTRACT

In this paper, a constant absolute bandwidth (CABW) band-pass filter based on magnetic dominated mixed coupling and source–load electric coupling is proposed. Specially, a novel mixed electric and magnetic coupling structure is presented to control the coupling coefficient variation and thus realize a narrow CABW width. Two transmission zeros are added to the filter response using a source–load coupling technique, leading to a better selectivity. The measurement shows that the −1 dB absolute and fractional bandwidth is 29 ± 3 MHz and 1.8–2.6%, respectively, while the central frequency of the passband varies from 1.11 to 1.51 GHz.

ARTICLE HISTORY
Received 12 April 2016
Accepted 17 August 2016

KEYWORDS
Tunable band-pass filter; constant absolute bandwidth; magnetic dominated mixed coupling; source–load electric coupling

1. Introduction

Tunable/reconfigurable microwave components are essential for future wideband wireless communication systems due to their abilities to adapt themselves to dynamic spectrum or reconfigurable applications,[1–7] and microwave tunable filters receive ever-increasing demands because of its ability to build the dynamic or multiband frequency channel and to improve the anti-jamming performance. Recently, magnetic dominated mixed coupling has been utilized to achieve a stable bandwidth. In [8], novel mixed coupled quarter-wavelength corrugated microstrip lines were used to design tunable filters with a 66–74 MHz −1 dB bandwidth. In [9], mixed coupled microstrip quarter-wavelength resonators loaded with varactor diode at the open end, as shown in Figure 1(a), were employed to design a three-pole tunable combline band-pass filter with 6–9.5 dB insertion loss and almost 50 MHz −1 dB bandwidth. In [10], mixed coupled half-wavelength resonators, as shown in Figure 1(b), were adopted to design frequency-agile band-pass filters with 1.6–2.0 dB insertion loss and 60 MHz −1dB bandwidth. However, it is clear that the −1 dB fractional bandwidth of these aforementioned filters is larger than 3%.

In this paper, magnetic dominated mixed coupled resonator is used to design the tunable filter with constant absolute bandwidth (CABW), as shown in Figure 1(c). One can see that an open-end microstrip line is connected to the tunable capacitor C_L. The open-end microstrip line can be equivalent to C_1, as shown in Figure 1(d). As C_L is connected to C_1 in series, the

CONTACT Quanyuan Feng fengquanyuan@163.com

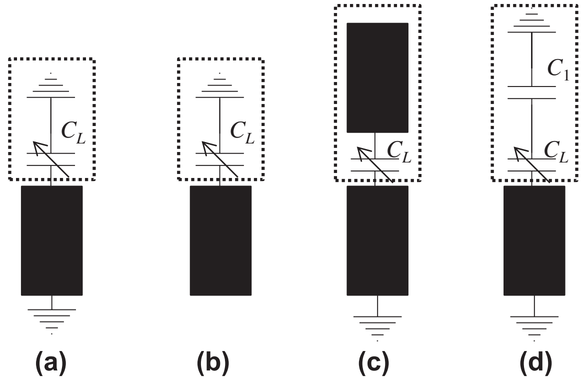

Figure 1. Four types of microstrip resonators.

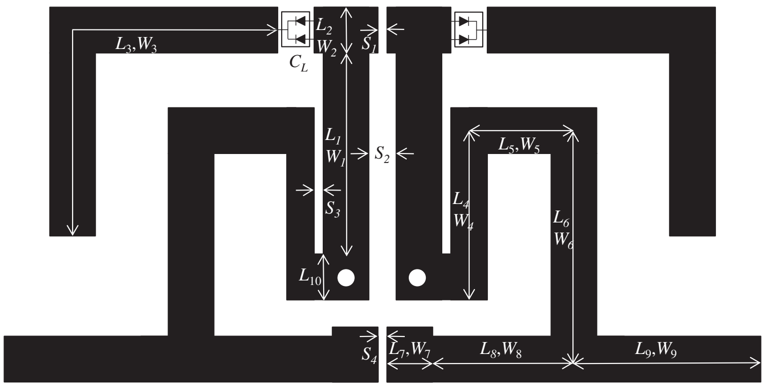

Figure 2. Layout of the proposed tunable band-pass filter with CABW.

tunable frequency range will be reduced. However, the insertion loss and the quality factor can be improved.[12] To improve the selectivity of the filter response, two transmission zeros are introduced using additional source–load coupling technique.[11] The attractive performances of the proposed constructers are validated by both theoretical analysis and experiment.

2. Filter configuration

Figure 2 shows the configuration of the proposed two-pole tunable band-pass filter with CABW. It consists of two resonators loaded with varactors, and the feeding lines with source–load coupling. Varactor diodes are used to tune the resonant frequency. The topology of the filter is depicted in Figure 3, where **S** is the source, **L** is the load, **E** is the electric coupling path, and **M** is the magnetic coupling path. The microstrip resonator is inductive when the working frequency of the resonator is higher than the resonant frequency, and the phase shift of the resonator is –90°.[12] On the other hand, the microstrip resonator is capacitive when the working frequency of the resonator is lower than the resonant frequency, and the phase shift of the resonator is +90°. Therefore, the phase difference between the signal

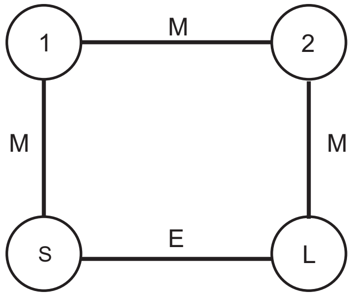

Figure 3. Magnetic dominated mixed coupling and source–load electric coupling topology of the proposed tunable band-pass filter.

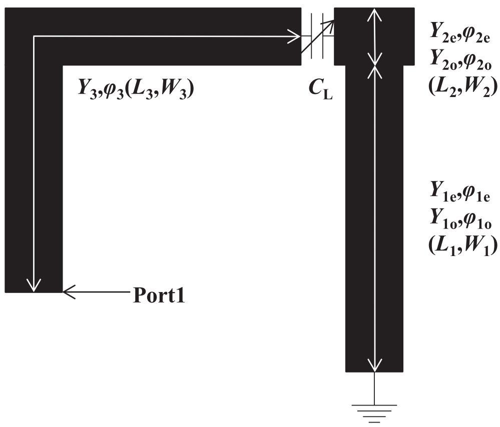

Figure 4. The electrical circuit model of the proposed resonant.

transmission path S-1–2-L and S–L can be 180° when the working frequency is lower and higher than the resonant frequency. Moreover, two transmission zeros can be created at the low-side and high-side bands, respectively.

3. Design of the tunable filter

3.1. Admittance matrix of the coupled resonators

Figure 4 shows that the electrical circuit model of the proposed resonant, the even-mode and odd-mode input admittances of the coupled resonator can be given as follows:

$$Yin_e = jY_3 \frac{(Y_3 \tan \varphi_3 + \omega C_L)A_{1e} - A_{0e}}{(Y_3 - \omega C_L \tan \varphi_3)A_{1e} + \tan \varphi_3 A_{0e}} \tag{1}$$

$$Yin_o = jY_3 \frac{(Y_3 \tan \varphi_3 + \omega C_L)A_{1o} - A_{0o}}{(Y_3 - \omega C_L \tan \varphi_3)A_{1o} + \tan \varphi_3 A_{0o}} \tag{2}$$

where A_{1e}, A_{0e}, A_{1o}, and A_{0o} can be obtained as follows:

$$A_{1e} = Y_{1e}\tan\varphi_{2e} + Y_{2e}\tan\varphi_{1e} \tag{3}$$

$$A_{0e} = Y_{2e}\left(Y_{1e} - Y_{2e}\tan\varphi_{1e}\tan\varphi_{2e}\right) \tag{4}$$

$$A_{1o} = Y_{1o}\tan\varphi_{2o} + Y_{2o}\tan\varphi_{1o} \tag{5}$$

$$A_{0o} = Y_{2o}\left(Y_{1o} - Y_{2o}\tan\varphi_{1o}\tan\varphi_{2o}\right) \tag{6}$$

Y_3 is the impedance of the microstrip line with width W_3, Y_{1e} and Y_{2e} are the even-mode impedance of the microstrip line with width W_2, Y_{1o} and Y_{2o} are the odd-mode impedance of the microstrip line with width W_1. Similarly, φ_3 is the electrical length of the microstrip line with length L_3, φ_{1e} and φ_{2e} are the even-mode electrical length, φ_{1o} and φ_{2o} are the odd-mode electrical length for each segments, C_L is the tunable capacitance. The overall admittance matrix of the capacity-loaded coupled resonators can be written as follows [13]:

$$Y = \begin{bmatrix} \frac{Yin_e+Yin_o}{2} & \frac{Yin_e-Yin_o}{2} \\ \frac{Yin_e-Yin_o}{2} & \frac{Yin_e+Yin_o}{2} \end{bmatrix} \tag{7}$$

3.2. Frequency control

Using Equation (7), the resonance condition is written as follows:

$$\mathrm{Im}[Y_{11}(\omega_0)] = 0 \tag{8}$$

where ω_0 is the central radian frequency.

Then, the resonance condition under different C_L can be get as follows:

$$B_2C_L^2 + B_1C_L + B_0 = 0 \tag{9}$$

where B_2, B_1, B_0 are given as follows:

$$B_2 = 2\omega^2 A_{1e}A_{1o}\tan\varphi_3 \tag{10}$$

$$B_1 = 2\omega[A_{1e}A_{1o}Y_3(\tan\varphi_3^2 - 1) - \tan\varphi_3(A_{0e}A_{1o} + A_{0o}A_{1e})] \tag{11}$$

$$B_0 = 2\tan\varphi_3(A_{0e}A_{0o} - Y_3^2A_{1e}A_{1o}) - Y_3(A_{0e}A_{1o} + A_{0o}A_{1e})(\tan\varphi_3^2 - 1) \tag{12}$$

The tunable frequency range can be calculated using Equation (9), as shown in Figure 5. It shows that the fractional tuning range increases when the length L_3 of the resonator decreases.

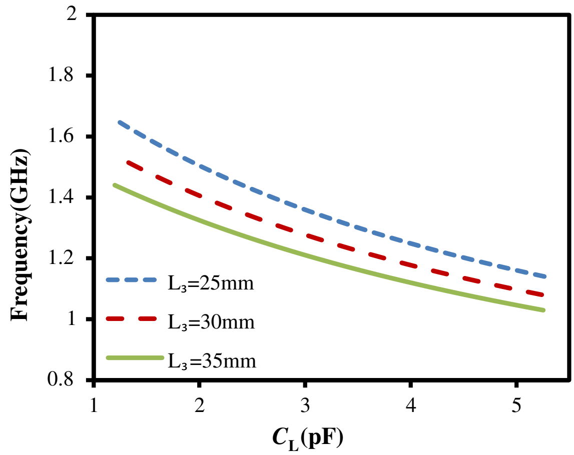

Figure 5. Resonant frequencies of the proposed resonator.

3.3. Bandwidth control

The coupling coefficient k_{12} can be obtained as follows:

$$k_{12} = \frac{\mathrm{Im}[Y_{12}(\omega_0)]}{b} = \frac{\mathrm{ABW}}{f_0\sqrt{g_1 g_2}} \tag{13}$$

where $b = \frac{\omega_0}{2}\frac{\partial \mathrm{Im}[Y_{11}(\omega_0)]}{\partial\omega}$, ABW is the absolute bandwidth, f_0 is the center frequency of the passband, g_1 and g_2 are the constant parameters for a specified filter response.

Therefore, the coupling coefficients must decrease, while the working frequency increases for the tunable filters with CABW. Using Equation (13), the coupling coefficient k_{12} can be calculated as shown in Figure 6. It shows that the slope of k_{12} can be modified to meet the requirements of the CABW by adjusting the ratios of L_1 and L_2 in the coupling structure.

3.4. External quality factor Q_{ext}

The external quality factor Q_{ext} is given as follows [14]:

$$Q_{\mathrm{ext}} = \frac{f_0 g_0 g_1}{\mathrm{ABW}} = \frac{2\pi f_0 \cdot \tau_{S_{11}}(f_0)}{4} \tag{14}$$

where τ_{S11} is the group delay.

To study the external quality factor of the filter, a half circuit of the filter is presented in Figure 7, which is simulated using *Sonnet*. The group delay τ_{S11} can be obtained via simulations. Figure 8 shows Q_{ext} for the filter response with a CABW. The value is 39–52 over the frequency range of 1.12–1.51 GHz.

3.5. Filter design and simulation

Figure 9 shows the configuration of the proposed filter. The design parameters of the filter can be determined using the above Equations (1)–(13). The parameters W_1, L_1, W_2, and L_2

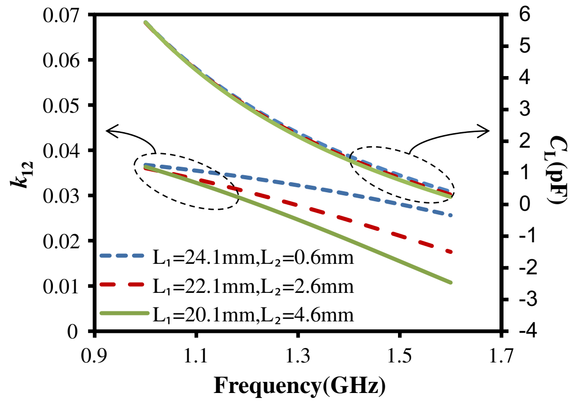

Figure 6. Coupling coefficient k_{12} and C_L under different resonant frequencies.

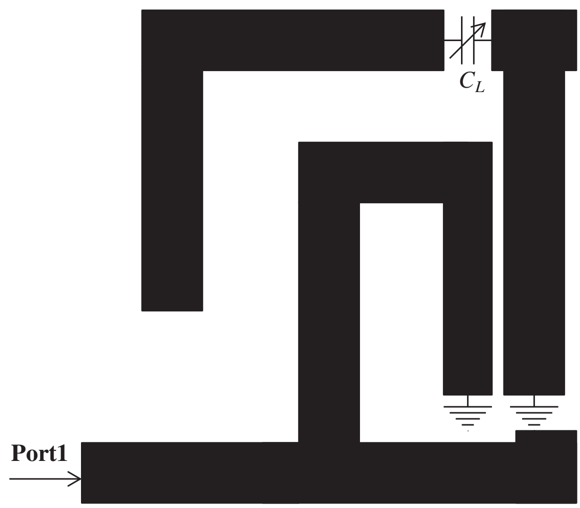

Figure 7. Simulation model of the tunable resonator for Q_{ext}.

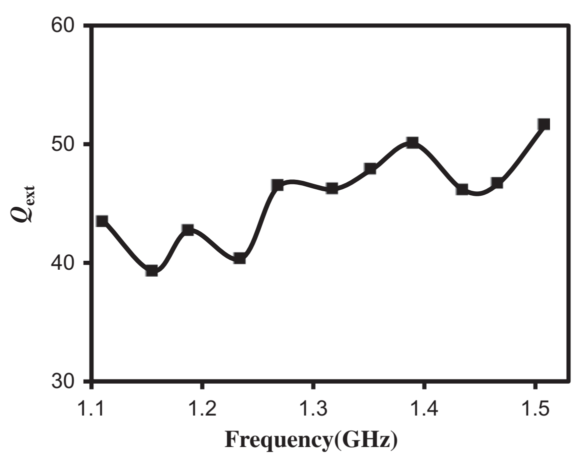

Figure 8. Simulated Q_{ext} variation with resonance frequency.

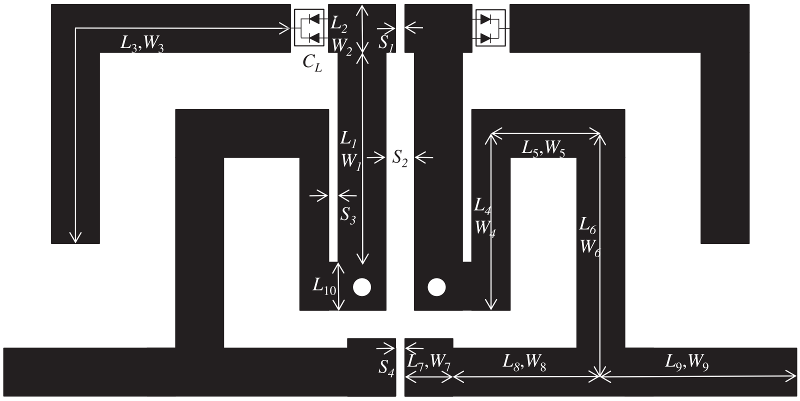

Figure 9. Configuration of the proposed tunable filter.

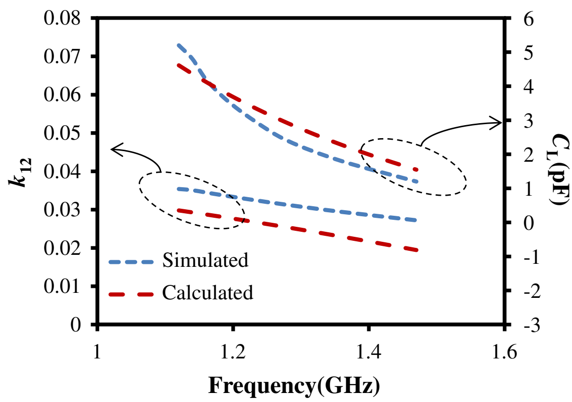

Figure 10. Simulated and calculated for the coupling coefficient k_{12} and C_L under different resonant frequency.

Table 1. Critical dimensions of the band-pass filter (Unit: mm).

L_1/W_1	L_2/W_2	L_3/W_3	L_4/W_4	L_5/W_5	L_6/W_6	L_7/W_7
19.1/2.6	2.6/4	29.1/2.6	17/1.2	3.4/3.3	22.4/2.9	3.3/3.7
L_8/W_8	L_9/W_9	L_{10}	S_1	S_2	S_3	S_4
5.4/2.4	21.2/2.4	3	0.2	1.8	0.3	0.4

can be chosen firstly to satisfy Equation (13), then the parameters W_3 and L_3 can be found using Equation (9). Table 1 is the critical dimensions of the band-pass filter.

The transmission responses for the proposed filter are simulated by *Sonnet* and *Agilent* ADS. The k_{12} can be obtained by the simulation using the Equation (15):

$$k_{12} = \frac{f_2^2 - f_1^2}{f_2^2 + f_1^2} \tag{15}$$

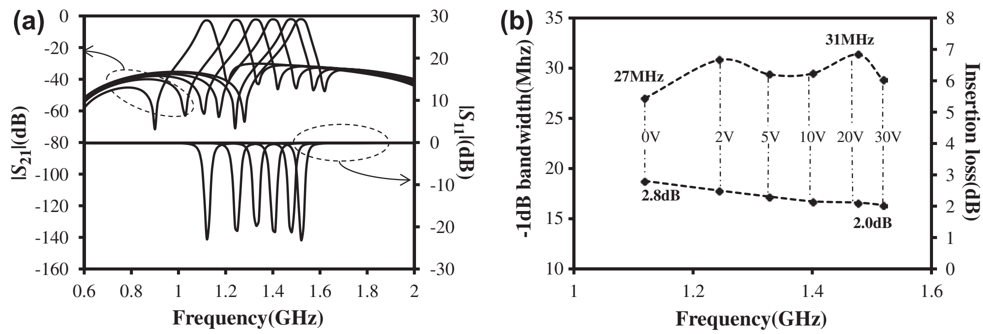

Figure 11. The EM simulated results: (a) the $|S_{21}|$ and $|S_{11}|$ under different C_L, (b) the center frequency −1 dB bandwidth and insertion loss of the tunable band-pass filter.

where f_1, f_2 are the two splitting resonant frequencies in the passband. Based on the weak coupling loading on both ends of the resonator, Figure 10 shows the simulated k_{12}. Clearly, the resonant frequency ranges from 1.12 to 1.51 GHz by adjusting C_L from 5.34 to 1.26 pF. Further, k_{12} decreases, while the resonant frequency increases.

Figure 11(a) and (b) shows the simulated response, bandwidth, and insertion loss of the configuration presented in Figure 9. SMV-1405 varactors from SKYWORKS in SC-70 package have been used as tuning elements. The single varactor capacitance is 0.63 and 2.67 pF under 30 and 0 V reverse bias voltage, respectively. By varying the bias voltage from 0 V to 30 V, the center frequency of the filter can be tuned from 1.12 to 1.51GHz with a −1 dB bandwidth in the range of 29 ± 2 MHz. The return loss is almost larger than 15 dB, and two transmission zeros are generated at the stopband, resulting in a sharp selectivity.

4. Experimental results

The filter shown in Figure 9 is fabricated on 0.8-mm F4B-2 substrate ($\varepsilon r = 2.65$, $\tan\theta = 0.001$), as shown in Figure 12. The core area is 50 mm × 59.8 mm, and each SMV-1405 varactor in SC-70 package is biased through 51-kΩ resistor. The *S*-parameters are measured using Agilent E5071C vector network analyzer.

Figure 13(a) shows the measured *S*-parameters, which agree well with the simulation. Figure 13(b) shows that the center frequency of the passband can be continuously tuned from 1.11 to 1.51 GHz and a 400 MHz tuning range can be attained. The −1dB absolute bandwidth is in the range of 29 ± 3 MHz, and the fractional bandwidth is in the range of 1.8–2.6%. Two transmission zeros are generated, leading to a sharp selectivity. The insertion loss of the passband is 3.6–4.2 dB, and the return loss is better than 10 dB over the whole tuning range. The input third-order intercept point (IIP3) is measured by Rohde & Schwarz FS300 spectrum analyzer and Agilent E4433B ESG-D series digital RF signal generator with 1-MHz frequency spacing. The measured IIP3 varies from 2.9 to 25 dBm, as shown in Figure 14. The comparation between the proposed filter and some recent designs is listed in Table 2. One can observe from Table 2 that the proposed filter has the minimum –1 dB bandwidth.

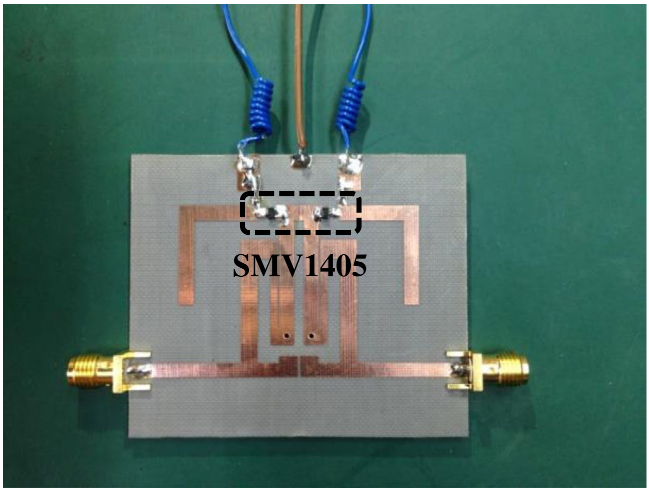

Figure 12. The photo of the fabricated band-pass filter.

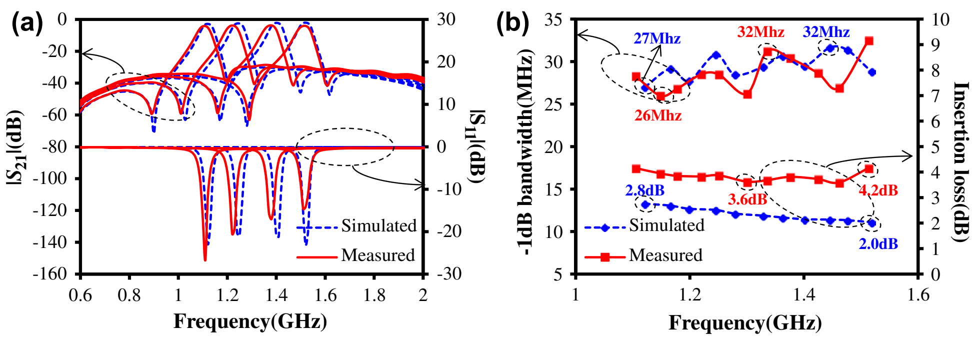

Figure 13. The measured results: (a) the $|S_{21}|$ and $|S_{11}|$, (b) −1 dB bandwidth and insertion loss.

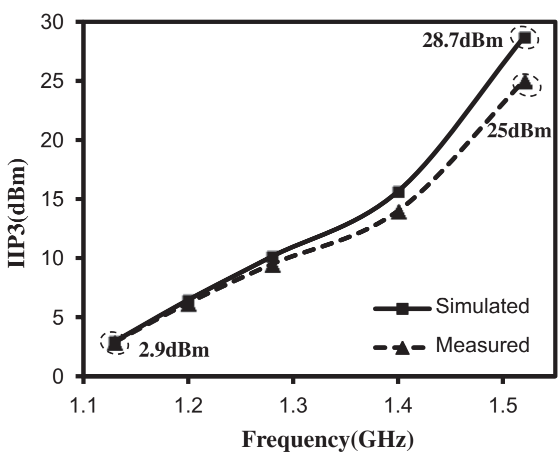

Figure 14. The EM simulated and measured IIP3 vs. the frequency of the filter.

Table 2. Comparison with related reference.

Design	f_0 (GHz)	−1dB bandwidth	Insertion loss (dB)	Tuning element (single)	IIP3 (dBm)
Chiou [9]	1.4–2.2	50 MHz, 2.3–3.5%	6–9.5	MA46H201(0.3–2 pF)	11–19
Zhang [10]	0.63–0.93	60 ± 3 MHz, 6.5–9.5%	1.6–2.0	1SV277(2–4.5 pF)	Around 13
	0.65–0.96	80 ± 3.5 MHz, 8.3–12.3%	1.2–1.5		
El-Tanani [15]	1.39–1.81	65–97 MHz, 4.6–5.4%	1.8–2.5	MA46H071(0.5–2 pF)	13.5–27.5
	1.52–1.95	67–105 MHz, 4.4–5.5%	1.25–2.9	MSV34064(0.9–3.4 pF)	26.5–41.5
Park [16]	0.803–1.335	5.1–5.7%	1.04–2.88	MA46H202(0.54–3 pF)	12–18.5
	0.911–1.335	43 ± 3 MHz, 2.9–5.2%	1.93–2.89		11.5–15
	0.86–1.41	4.3–6.5%	1.18–3.47		11–20
This work	1.11–1.51	29 ± 3 MHz, 1.8–2.6%	3.6–4.2	SMV1405(0.63–2.67 pF)	2.9–25

5. Conclusion

In this paper, a novel CABW tunable band-pass filter with mixed electrical and magnetic coupling has been designed and demonstrated. The measured results show that the −1dB absolute bandwidth varies is 29 ± 3 MHz and the −1dB fractional bandwidth is 1.8–2.6% while the central frequency of the passband varies from 1.11 to 1.51 GHz. Source–load coupling is introduced to generate transmission zeros, which can improve frequency selectivity performance. The stopband characteristics of the fabricated filter are more than −25 dB up to 2 GHz over the entire tuning range of the passband.

Disclosure statement

No potential conflict of interest was reported by the authors.

Funding

This work was supported by National Natural Science Foundation of China [grant number 61271090], [grant number 61401375], [grant number 61531016]; Science and Technology Foundation of Sichuan Province [grant number 2015GZ0103]; Central University Foundation under [grant number 2682014RC24], [grant number 2682015CX065].

References

[1] Hsiao PY, Weng RM. Compact tri-layer ultra-wideband bandpass filter with dual notch bands. Prog. Electromagnet. Res. 2010;106:49–60.
[2] Xu J, Li B, Wang H, et al. Compact UWB bandpass filter with multiple ultra narrow notched bands. J. Electromagnet. Waves Appl. 2011;25:987–998.
[3] Tombak A, Maria J-P, Ayguavives FT, et al. Voltage-controlled RF filters employing thin-film barium–strontium–titanate tunable capacitors. IEEE Trans. Microwave Theory Tech. 2003;51:462–467.
[4] Keane WJ. Narrow-band YIG filters aid wide open receivers. Microwaves. 1978;17:50–54.
[5] El-Tanani MA, Rebeiz GM. High-performance 1.5–2.5-GHz RF-MEMS tunable filters for wireless applications. IEEE Trans. Microwave Theory Tech. 2010;58:1629–1637.
[6] Koochakzadeh M, Abbaspour-Tamijani A. Tunable filters with nonuniform microstrip coupled lines. IEEE Microwave Compon. Lett. 2008;18:314–316.
[7] Dussopt L, Rebeiz GM. Intermodulation distortion and power handling in RF MEMS switches, varators, and tunable filters. IEEE Trans. Microwave Theory Tech. 2003;51:1247–1256.
[8] El-Tanani MA, Rebeiz GM. Corrugated microstrip coupled lines for constant absolute bandwidth tunable filters. IEEE Trans. Microwave Theory Tech. 2010;58:956–963.

[9] Chiou Y-C, Rebeiz GM. A tunable three-pole 1.5-2.2 GHz bandpass filter with bandwidth and transmission zero control. IEEE Trans. Microwave Theory Tech. 2011;59:2872–2878.
[10] Zhang X-Y, Xue Q, Chan C-H, et al. Electrical tunable microstrip LC bandpass filters with constant bandwidth. IEEE Trans. Microwave Theory Tech. 2010;58:1557–1564.
[11] Amari S. Direct synthesis of folded symmetric resonator filters with source–load coupling. IEEE Microwave Compon. Lett. 2001;11:264–266.
[12] Sabbagh ME, Zaki KA, Yao H-W, et al. Full-wave analysis of coupling between combline resonators and its application to combline filters with canonical configurations. IEEE Trans. Microwave Theory Tech. 2001;49:2384–2393.
[13] Park S-J, Van Caekenberghe K, Rebeiz GM. A miniature 2.1-GHz low loss microstrip filter with independent electric and magnetic coupling. IEEE Microwave Compon. Lett. 2004;14:496–498.
[14] Hong JS, Lancaster MJ. Microstrip filters for RF/microwave applications. New York, NY: Wiley; 2001.
[15] Park S-J, Rebeiz GM. A tunable combline bandpass filter loaded with series resonator. IEEE Trans. Microwave Theory Tech. 2009;57:830–839.
[16] Park S-J, Rebeiz GM. Low-loss two-pole tunable filters with three different predefined bandwidth characteristics. IEEE Trans. Microwave Theory Tech. 2008;56:1137–1148.